



AD-A175 931

C S S A

DISTRIBUTION OF FLARES ON THE SUN:
SUPER ACTIVE REGIONS AND
ACTIVE ZONES OF 1980-1985

TAEIL BAI

Center for Space Science and Astrophysics, Stanford University

CSSA-ASTRO-86-31

May 1986



DTIC
ELECTE
JAN 12 1987
S D

CENTER FOR SPACE SCIENCE AND ASTROPHYSICS
STANFORD UNIVERSITY
Stanford, California

DTIC FILE COPY

DISTRIBUTION STATEMENT A
Approved for public release
Distribution Unlimited

86 12 18 01

8

DISTRIBUTION OF FLARES ON THE SUN:
SUPER ACTIVE REGIONS AND
ACTIVE ZONES OF 1980-1985

TAEIL BAI

Center for Space Science and Astrophysics, Stanford University

✓
CSSA-ASTRO-86-31

May 1986

DTIC
ELECTE
JAN 1 2 1987
S D D

National Aeronautics and Space Administration Grant NGL 05-020-272
Office of Naval Research Contract N00014-85-K-0111

DISTRIBUTION STATEMENT A

Approved for public release
Distribution Unlimited

DISTRIBUTION OF FLARES ON THE SUN:
SUPER ACTIVE REGIONS AND ACTIVE ZONES OF 1980 - 1985

Taeil Bai

Center for Space Science and Astrophysics, Stanford University

Received 1986 May 9; accepted 1986

ABSTRACT

I have analyzed coordinates of energetic solar flares observed with the Hard X-Ray Burst Spectrometer ^{over an analysis period} during the period from 1980 February through 1985 August. Important discoveries resulting from this analysis are as follows: (1) A small number (28) of "super active regions" produced the majority of the major flares during this period. These super active regions are large, complex active regions containing large sunspots. (2) There exist active zones, in which the flare occurrence rate is much higher. Two active zones are in the northern hemisphere, and two in the southern hemisphere. The longitudinal separation of the two active zones in the same hemisphere is about 180 degrees, but the active zones of the southern hemisphere are misaligned from those of the northern hemisphere by about 80 degrees. The rotation period of the active zones is 26.75 days. Active zones last several years or longer. (3) There is a hint of active centers rotating at a period of 23.7 days. It is possible that active centers in deep layers rotate with such a period. *Key words: solar flares, solar activity, solar rotation, solar X-rays*

Subject headings: Sun: activity—Sun: flares—Sun: rotation—Sun: X-rays

- 1 -



Accession For	
NTIS CRA&I	<input checked="checked" type="checkbox"/>
DTIC TAB	<input type="checkbox"/>
Unannounced	<input type="checkbox"/>
Justification	
By <i>lth on file</i>	
Distribution /	
Availability Codes	
Dist <i>A-1</i>	Avail and/or Special

I. INTRODUCTION

It is important to determine whether solar flares occur uniformly all over the solar longitudes or preferentially at some longitudes. For such information may enhance our understanding of the solar activity. Even in very early days of solar physics, Carrington (1863) suspected that sunspots did not form randomly over the solar longitudes. Bumba and Howard (1965) showed that series of active regions occur preferentially in certain regions on the Sun, which rotate at about the Carrington rate. Such regions were called "complexes of activity." "Evolutionary charts" of calcium plages plotted by Hedeman, Dodson, and Roelof (1981) show the existence of complexes of activity. More recently, Gaizauskas *et al.* (1983) confirmed the existence of complexes of activity, by studying the evolution of magnetic polarity patterns.

Lifetimes of complexes of activity are order of several months. For longer timescales, Warwick (1965) studied the distribution of 77 proton flares that had caused polar-cap absorption (PCA) during 1954-1963. Warwick (1965) proposed that there exist two active intervals of heliographic (Carrington) longitudes where the occurrence rate of proton flares is higher. By studying the coordinates and evolutionary charts of the 7 active regions that produced 10 proton flares during 1963 through 1967, Svestka and Simon (1969) and Svestka (1970) found that most of them were located in one interval of Carrington longitudes. Such intervals of Carrington longitudes of high flare activity are called "active longitudes" (see reviews by Svestka 1976; McIntosh 1981). However, the numbers of flares studied in the above papers are rather small to be impressive. Furthermore, seeing the evolutionary charts of active regions made by Hedeman, Dodson, and Roelof (1981), one can hardly discern the existence of active longitudes which persist for many years. Therefore, the reality of active longitudes has not been widely

accepted, even though its concept has been around for several decades. For this reason, it is important to study the existence of active longitudes for solar cycle 21, which has been observed in detail with the Solar Maximum Mission (*SMM*) and other ground-based observatories. One of the aims of this study is to investigate the existence of active longitudes.

Another aim of this paper is to identify active regions which produced large numbers of energetic flares. Determination of the characteristics of such active regions will be helpful to both understanding the cause of flares and predicting flares.

A study of flare locations on the Sun can also yield a valuable clue to the underlying mechanism of the recently-discovered 152-day periodicity of flare occurrence (Rieger *et al.* 1984; Kiplinger *et al.* 1984; Bogart and Bai 1985). This will be a subject of our forthcoming paper.

The plan of this paper is as follows. I am going to discuss the data base in §II. For this paper I mainly study the locations of "major flares," which are defined as flares with Hard X-Ray Burst Spectrometer (HXRBS) peak count rates exceeding 1000 counts s^{-1} . In §III, I am going to show that the majority of major flares of the 1980-1985 period were produced by a relatively small number (28) of "super active regions." The properties of these super active regions are briefly discussed in this section. In §IV, I am going to demonstrate that the flare occurrence rate is higher in active zones, which rotate with a period of 26.75 days. (All the rotation periods appearing in this paper are synodic periods.) This period is shorter than the Carrington period (27.2753 days) by $\sim 2\%$. Implication of this finding is discussed here. In §V, it will be shown that a large number of super active regions have similar longitudes in a frame rotating at a constant rate of 23.7 days. This

could be due to activity sources in the deep layer rotating at that rate. In §VI, summary and conclusions are provided.

II. DATA BASE

As a main data base for this study, I use the flares that were observed with *SMM* during the period from its launch in 1980 February to 1985 August, and whose hard X-ray peak fluxes measured with HXRBS exceed 1000 counts s^{-1} . Out of $\sim 7,800$ solar flares observed with HXRBS during this period, 485 flares are found to have HXRBS peak rates ≥ 1000 counts s^{-1} (Dennis *et al.* 1985). The peak hard X-ray fluxes give a good measure of energy release rates during the impulsive phase of flares; thus these 485 flares represent fairly energetic flares. For convenience I call these flares major flares. The number of major flares for this study is large enough to be meaningful and small enough to be manageable.

The GOES classification scheme, based on the 1–8 Å soft X-ray peak flux, is widely used. It seems appropriate to compare with the GOES classes for those who are accustomed to them. The GOES classes of flares with HXRBS peak rates between 1000 and 2000 counts s^{-1} range from C1 to M9, and the median is M1.

For the determination of positions of these flares I used Comprehensive Reports of the *Solar Geophysical Data* (*SGD*) for flares observed until the end of 1983, and Prompt Reports of the *SGD* for flares observed afterwards. As usual, the time coincidence is used for association with $H\alpha$ flares. Because the flares under consideration are energetic, $H\alpha$ flare association can be made unambiguously for most cases. The locations of 43 major flares could not be determined mainly because $H\alpha$ patrol observations were not available. I also use the *SGD* for tracing the family trees of active regions.

III. SUPER ACTIVE REGIONS

During the period from 1980 February to 1985 August, about 2300 active regions appeared on the visible solar disk. Only 163 regions out of these ~2300 active regions were found to produce major flares. (Some active regions are known to persist for several solar rotations; but at each passage new active region numbers are assigned, and my estimate is based on active region numbers.) Of these 163 active regions, 28 were observed to produce five or more major flares. Considering their high productivity of major flares, we may call these active regions "super active regions." These 28 super active regions produced 234 major flares, accounting for 53 % of all the major flares with identified active regions.

Figure 1 shows number of active regions vs. number of major flares per active region. The actual data are shown by the histogram, and two cases of the Poisson distribution are shown with solid dots and squares, for comparison. The Poisson distribution is given by

$$y(n) = A \frac{\lambda^n}{n!} e^{-\lambda}.$$

The solid dots represent the case for $\lambda=0.6$ and $A=270$; solid squares, $\lambda=5$ and $A=40$. Eighty-six active regions are found to produce only one major flare each while *SMM* was observing the Sun; on the other hand, several active regions are found to produce more than 10 major flares. Because *SMM* is in the Earth's shadow approximately 50 % of the time, the actual rates should be regarded as about double the rates shown in this figure.

In Table 1 super active regions are listed chronologically, showing some pertinent properties. Active region 18405 (NOAA region number 3763) produced the largest number (17) of major flares, making 1982 June the most active month in terms of major flare production. During the same month, active region 18422

(NOAA region number 3776) produced 15 major flares, and it was still very active during its next passage across the disk (active region number 18474; NOAA region number 3804), producing 13 major flares. In this Table the maximum of total sunspot areas of each active regions (in 10^{-6} solar disk) reported in the *SGD* are listed. Super active regions are all very large with total sunspot areas exceeding 500 millionth of the disk. McIntosh classification symbols for active regions (McIntosh 1981, 1986) are also listed for the day when the total sunspot area of each active region was maximum. The first of the classification symbols represents the total sunspot area of the active region (area increasing with *A*, *B*, *C*, *D*, *E*, *F*). The second letter indicates the size of the largest sunspot in the active region, with the letters *x*, *r*, *s*, *a*, *h*, and *k* representing increasingly larger sunspots. All the super active regions with available information are found to contain very large sunspots corresponding to class symbol *k*. The last of the classification symbols represents the sunspot distribution. The letters *x*, *o*, *i*, and *c* represent progressively complex active regions. Most of super active regions have *i* or *c* as third classification symbols, indicating that they are complex active regions. In summary, super active regions are large and complex active regions containing very large spots as their constituents. This is not very different from the conventional wisdom. The flare occurrence rates for each of the three classification symbols have been studied, and the following result has been found (McIntosh 1986). The flare occurrence rate is highest when the first of the three classification symbols is *F*, when the second symbol is *k*, and when the third is *c*, respectively.

In order to learn more about the properties of the super active regions, one should study them in detail using magnetograms and optical observations, which is beyond the scope of the present paper.

IV. ACTIVE ZONES

a) Northern Hemisphere

According to the concept of "active longitudes," solar flares occur more frequently in certain intervals of longitudes, which rotate at about the Carrington rate, than in other longitudes (cf. Svestka 1976). In order to investigate the existence of active longitudes, I have performed the following procedure. First, adopt a coordinate system rotating at an assumed constant rate (synodic) about the solar axis to the same direction as the actual solar rotation. (A constant sidereal solar rotation rate is not converted into a constant synodic solar rotation rate because of the finite eccentricity of the Earth orbit. However, the eccentricity is small enough to be negligible for the present purpose.) As the zero longitude, take the Eastern solar limb at 00:00 UT on 1980 January 1. Then, the angular separation of the zero longitude from the Eastern limb is given as a function of time and assumed rotation period P :

$$l_0(t, P) = \{ t/P - INT(t/P) \} 360, \quad (1)$$

where t is the time elapsed since 00:00 UT on 1980 January 1. The relative longitude of a flare in this frame is expressed by

$$l_{rel}(l_f, t, P) = \begin{cases} l_f - l_0, & \text{if } l_f \geq l_0; \\ l_f - l_0 + 360, & \text{otherwise.} \end{cases} \quad (2)$$

where l_f is the longitudinal distance of the flare from the Eastern limb. Then, calculate the relative longitudes of all the major flares with known positions, and calculate the numbers of flares in twelve 30-degree longitude bins for northern and southern hemispheres separately. The bin size was chosen to be 30 degrees because

large active regions extend 30 degrees or more in longitudes. Then, calculate the variance of the flare distribution in these bins, where the variance S^2 is defined as

$$S^2 = \frac{\sum_{i=1}^{12} (N_i - \bar{N})^2}{11}. \quad (3)$$

Here N_i is the number of flares in the i th bin, and \bar{N} is the mean flare number per bin. Here I use 11 in the denominator instead of 12 the bin number, because this gives a statistically unbiased estimate of the variance (cf. Brandt 1976). The RMS deviation S is the square root of the variance.

Obviously, the variance will be a function of assumed period. If there exist active longitudes, the variance obtained in this way will show a significant peak near the rotation period of the active longitudes when it is plotted as a function of assumed rotation period. Figure 2 shows the RMS deviation as a function of assumed rotation period, for the major flares observed in the northern hemisphere from 1980 February to 1985 August. Here we can see a prominent peak at 26.75 days. For a given periodicity, the variance depends, for a small degree, on the starting point of the first bin, α . I have tried ten values of α , 0, 3, 6, ..., 27 degrees to find that peak A is largest when α is 6 degrees. (Depending on the choice of α , the peak position of the period ranges from 26.72 to 26.77 days.)

Figure 3 shows the histogram for flare number distribution in a frame rotating with a period of 26.75 days. Eighty-six (86) flares, which is more than five times the mean value or 43 % of all the northern hemisphere flares, are concentrated in the 216–246 degree bin. The distribution shown in Figure 3 is really impressive. However, the period 26.75 days is shorter than the Carrington period (27.2753 days) by ~ 2 %. This difference is substantial. The same position in a frame rotating at 26.75 days will experience a 360 degree drift in Carrington longitudes

in less than four years, which is shorter than the time period under investigation. Therefore, it is important to assure that 26.75 days is due to a real physical rotation.

In order to check whether 26.75 days corresponds to a real rotation of the active longitudes, I have studied family trees of important active regions appearing in the northern hemisphere. In Figure 4, I plot central meridian passage (CMP) dates and relative longitudes of active regions. The study of family trees of active regions is limited to the time until 1982 July because rotational relationship between active regions have been reported in the *Solar Geophysical Data* only until that time. Here the horizontal axis represents the relative longitude in a frame rotating with a 26.75 day period. Rotational relationships between active regions are shown with lines: a solid line indicates that the same active region re-appeared during the following rotation, and a dashed line indicates that the earlier active region disappeared with another active region appearing during the following rotation at the same location. If the interval between the successive CMP dates of the same active region is longer than 26.75 days, the line connecting them is tilted toward the left. If shorter, toward the right. Although many "branches" of active-region family trees are tilted to the left, the "stems" of long-lived active-region family trees are more or less vertical. This indicates that 26.75 days indeed represents the rotation of long-lived active regions. We can see two active zones — one in the 210–250 degree interval which includes 6 super active regions and several active regions with major flares and the other in the 10–50 interval which includes one super active region and several active regions with major flares. These two active zones are separated by approximately 180 degrees (cf. Fig. 3).

In Figure 4, horizontal grid lines are separated by 152 days. In agreement with a recently discovered 152-day periodicity in flare occurrence (Rieger *et al.*

1984; Kiplinger *et al.* 1984; Bogart and Bai 1985; Ichimoto *et al.* 1985), many of the super active regions are located just above the horizontal grids. The relation between the 152-day periodicity and flare locations on the Sun is a subject of a forthcoming paper.

We have seen that the longitudinal distribution in a frame rotating with a period of 26.75 days is highly non-uniform. If the major flares studied here are independent of each other, the statistical significance of flare concentration in active zones can be estimated by comparing the variance with the expected variance for a uniform distribution. But as we have seen in §III, some active regions produced large numbers of major flares. Therefore, a chance clustering of a small number of super active regions can cause a concentration of a large number of flares. I can think of the following three ways of estimating the significance of the flare concentration.

First, I have performed Monte Carlo simulations as follows. Because all the northern hemisphere major flares were produced by 79 active regions during 1980 February through 1985 August, I have randomized the CMP times of the 79 northern hemisphere active regions, according to random numbers uniformly distributed in the time interval 50–2070 days. The number of flares per active region was chosen to match the actual data. Flares from the same active region are made to be distributed randomly in a 10 degree longitudinal bin around the central position of the active region. For some active regions, the longitudinal extent of flare distribution is up to 20 degrees; thus, the choice of 10 degree is a conservative measure. Then, I have calculated flare distributions as a function of longitudes for rotation periods of every 0.01 day intervals in the range from 22 to 34 days. Then, I have calculated S , RMS deviation of flare numbers per bin, for each periods, using equation (3). The distribution of S values thus obtained

can be represented reasonably well by a Gaussian distribution. For the northern hemisphere, the mean value of S is about 9.0 and one standard deviation of S is about 1.90. The mean value and the standard deviation of S are found to be stable from one simulation to next. Therefore, the S value 22.5 for 26.75 days is significant at about the 7σ level. $[(22.5-9.0)/1.90 = 7.1]$

Second, we can find from Table 1 that 6 out of the 9 northern hemisphere active regions are in the 216-246 degree bin. In estimating the significance we can use the binomial probability distribution (cf. Brandt 1976). The formula

$$W(n, k, p) = \frac{n!}{k!(n-k)!} p^k (1-p)^{(n-k)}, \quad (4)$$

gives the probability that we will succeed k times out of n tries when the success ratio is p . Substituting $n = 9$, $p = (\frac{30}{360}) = 0.083$, and $k=6, 7, 8, 9$, we find that

$$\sum_{k=6}^9 W(9, k, 0.083) = 2.25 \times 10^{-5}.$$

However, we have freedom to choose the location of the bin. When the center of the 30 degree bin is any where between 226 and 236, 6 super active regions are found in the bin. Out of all possible locations of the center of the bin, this portion is $10/360$. Therefore, the probability that 6 out of the 9 northern hemisphere super active regions fall in the 30 degree bin by chance is given by

$$P = 2.25 \times 10^{-5} \times \frac{360}{10} = 8.1 \times 10^{-4}.$$

Third, we can investigate with the actual data the flare distributions in systems rotating with periods far different from 27 days. I have studied the flare

distributions in systems rotating with periods between 15 and 23 days and between 34 and 50 days and calculated S , the rms deviations about the mean flare number (cf. equation 3). It is found that the mean value of S is 6.77 and the standard deviation of S is 1.55 for the northern hemisphere. The largest value of S was found to be only 11.3. Both the mean and the standard deviation of S are less than the results of Monte Carlo simulations discussed above. The reason for this is that in systems rotating with periods far from 27 days distributions of active regions are not truly random. At any rate, the value 22.5 of S for 26.75 day rotation seems very extraordinary.

Judging from the above three estimates, the flare concentration shown in Figure 3 is statistically very significant.

b) Southern Hemisphere

Figure 5 shows family trees of active regions for the southern hemisphere, similarly to Figure 4. In this figure are plotted family trees of all the super active regions that appeared in the southern hemisphere between 1980 January and 1982 December. A few long-lived active regions (5 or 6 rotations) are also shown here to guide the eye. Again we can see two zones of active longitudes — one in the 90-150 degree interval and another in the 260-320 degree interval. The two zones are separated by about 180 degrees. Figure 6 shows a histogram for the flare distribution along the longitude.

Figure 7 is equivalent to Figure 2, for the southern hemisphere. We find that this figure is much noisier than Figure 2. Although we find a peak at 26.78 days (peak *A*), there are many peaks bigger than this peak. For example, peaks *C* and *D* at 26.28 and 27.28 days are bigger than peak *A*. Because the position of peak *D*, 27.28 days, is very close to the Carrington period, I plot in Figure 8 family trees

of active regions, using the Carrington longitude as the X -axis. We find 7 super active regions in the 60–120 degree Carrington longitude bin and 4 in the 285–345 degree bin, in consistence with the large peak D . Nevertheless, we can see in this figure that the “stems” of family trees are in general tilted toward the right. In contrast, in Figure 5 we can find that the stems of long-lived active-region family trees are more or less vertical, indicating that only peak A is due to a real rotation.

Let us follow the three methods of estimating the significance of the flare concentration shown in Figure 5. First, according to Monte Carlo simulations which were explained earlier, the mean value of S is about 10.6, and the standard deviation of S is about 2.25 for the southern hemisphere. Therefore, peak A is significant at the 2σ level. $[(15.-10.6)/2.25 = 1.96]$ Second, we can use the binomial probability as we did for the northern hemisphere. In two 60-degree intervals separated by 180 degrees (centered around about 100 and 280 degrees) are located 12 or 13 of the 19 southern hemisphere super active regions. Using the same argument as for the northern hemisphere, I find that the probability of chance clustering of such large numbers of super active regions is only 7.4×10^{-2} . Third, for systems rotating with periods between 15 and 23 days and between 34 and 50 days, the mean and the standard deviation of S are found to be 7.65 and 1.97. From the above estimates, we find that the statistical significance of the two active zones of the southern hemisphere is lower than that of the prominent active zone of the northern hemisphere. Nevertheless, the probability that they are due to random chance is quite low.

c) Discussion

By plotting the distribution of proton flares along Carrington longitudes for cycle 19 (1954–1963), Warwick (1965) showed that the distribution is not

uniform, and thereby proposed that the rotation period of active longitudes is the same as the Carrington period (27.2753 days). Studying the locations of active regions producing proton flares for the period of 1963–1967, Svestka and Simon (1969) showed that proton flares occur in rather small regions of the solar surface. By interpolating the regions of proton flare production, they also proposed that active longitudes rotate at about the Carrington rotation rate. Bumba and Obridko (1969) studied the relation between the CMP dates of active regions producing proton flares and interplanetary sector boundaries, and found that proton flares tend to occur in active regions whose CMP dates are close to those of the interplanetary sector boundaries.

The present study confirms the existence of active zones. We have shown that the rotation period of the active zones is 26.75 days, by studying the rotational relationship of families of active regions and by variance calculations. In Figure 9 are plotted flare locations in the frame rotating with 26.75 day period. We can find that the active zones of the southern hemisphere are not in the same longitude bands as those of the northern hemisphere. Therefore, the term “active longitudes” is a misnomer; a better term is “active zones.”

The rotation period determined in this study, 26.75 days, is different from the Carrington period, which was also proposed to be the period of active longitudes by Warwick (1965) and Svestka and Simon (1969). Let us investigate the cause of this discrepancy. Warwick did not deduce the rotation rate from the flare data but assumed the Carrington rate as the solar rotation rate in plotting the longitudinal distribution of flares. Svestka and Simon (1969) did plot the family trees of active regions that produced proton flares, similarly to Figures 4 and 5. But there were only 7 families of active regions during the five year period from 1963 January

to 1967 December, and only one active region produced a proton flare in the 23-month period near the solar minimum (1964 February–1965 December); therefore, the interpolation they made to determine the rotation period of the active zone is not unique.

Recently, Howard, Gilman, and Gilman (1984) studied rotation rates of sunspots and sunspot groups, using the Mount Wilson sunspot observations of the period from 1921 through 1982. The formula for sidereal rotation rates for spot groups for the 62 year interval was determined to be

$$\omega = 14.393(\pm 0.010) - 2.946(\pm 0.090) \sin^2 B \text{ deg day}^{-1},$$

where B is the heliographic latitude. The rotation rates determined for all spots are expressed by

$$\omega = 14.522(\pm 0.004) - 2.840(\pm 0.043) \sin^2 B \text{ deg day}^{-1}.$$

Scherrer, Wilcox, and Svalgaard (1980) determined from Doppler gram observations made at the Wilcox Stanford Solar Observatory that the rotation rates are expressed by

$$\omega = 14.44 - 1.98 \sin^2 B - 1.98 \sin^4 B \text{ deg day}^{-1}.$$

The synodic rotation period 26.75 days corresponds to the sidereal rotation rate $14.44 \text{ deg day}^{-1}$. Considering that a large fraction of the flares are in the 5–20 degree latitudinal bands, the rotation rate found in this paper is somewhat faster than the result obtained by Howard, Gilman, and Gilman (1983) for all sunspot groups. (However, it is comparable to their result for all spots.) The ensemble average of the intervals between CMP times at successive disk passages of the same active regions shown in Figure 4 (northern hemisphere) is 27.03 days, and it

happens to be exactly the same for Figure 5. Therefore, the rotation period 26.75 days (sidereal rotation rate $14.44 \text{ deg day}^{-1}$) is not the mean rotation period of active regions, but it represents the rotation period of sub-surface sources of activity. Hence, we can interpret that the average rotation rate of spot groups is slower than that of sub-surface activity sources, but that long-lived active regions and super active regions rotate at rates similar to that of sub-surface activity sources.

McIntosh (1981) showed that large-scale magnetic polarity patterns of the Sun are stable for several years (Figs. 22 and 23), and he proposed magnetic fields originating from sub-surface sources as a probable cause of such magnetic patterns. From Figure 22 of McIntosh (1981) one can determine the rotation period of the magnetic patterns of the equatorial strip (N20-S20) to be about 26.78 days, which is very close to what is found in this paper.

McIntosh and Wilson (1985) argued that these large-scale magnetic patterns are due to giant convection cells, whose existence has been speculated (Weiss 1964). McIntosh and Wilson proposed that the up-drafting boundaries of giant convection cells may carry magnetic fields from the interior of the Sun, and thus become the seats of many important active regions. If there are 8 giant cells girdling the equatorial belt, 4 cell boundaries are up-drafting regions and 4 down-drafting. McIntosh (1981) showed that active regions in general appear at magnetic polarity boundaries, but only at the boundaries where the large scale polarity is the same as the Hale's polarity law for sunspots. Then out of the 4 up-drafting boundaries, only two can satisfy the Hale's polarity law. Also the boundaries satisfying the Hale's polarity law are not the same for the northern and southern hemispheres. This may be the reason why the active zones of the two hemispheres are misaligned by 90 degrees. This picture is worth studying further in the future.

As we can see from Figure 4 and 5, active zones are not always active even during solar maximum years. One activity complex (prominent active region family) arises and disappears in an active zone, then some time later another activity complex arises in the same active zone. If the magnetic fields of activity complex are brought from deep layers of the convection zone, the lifetimes of activity complexes represent the timescale of exhausting the magnetic fields. Important active regions which produced 3 or more major flares are plotted in Figure 10. Large circles represent super active regions, and small circles represent active regions with 3 or 4 major flares. Filled circles are for the southern hemisphere; open circles, northern hemisphere. From 1983 the flare activity became rather low, especially in the northern hemisphere. However, a northern hemisphere active region which produced 4 major flares in 1985 appeared in the prominent active zone of the northern hemisphere. Similarly, the 3 super active regions appearing in the southern hemisphere since 1983 were located in one of the active zones. Hence, we can conclude that the lifetimes of active zones are of the order of several years. We cannot rule out the possibility of their lifetimes being longer than the present data base.

Because Carrington longitudes are often used in mapping solar surface phenomena, it is convenient to have the expression for the relation between the Carrington longitudes and the relative longitudes used in this paper. It can be shown that the same spot in a system rotating with a period of 26.75 days drift forward in Carrington longitudes by $0.259 \text{ degree day}^{-1}$ or 7.07 degree per Carrington rotation. It can be shown that

$$l_{rel}(t) = l_C(t) - 0.259t - 218 + 360n, \quad (5)$$

where t is time after 00 UT on 1980 January 1. Equivalently,

$$l_C(C) = l_{rel} + (C - 1690)7.07 + 218 - 360n, \quad (6)$$

where C is the Carrington rotation number, n is an integer to make the above value to be in the 0–360 degree range. By substituting $l_{rel}(t) = 230$ into the above equations, we can find the Carrington longitude of the center of the prominent active zone of the northern hemisphere. For other active zones, one should substitute for $l_{rel}(t)$ corresponding values, which can be found from Figures 3–6.

V. ROTATION WITH A PERIOD OF 23.7 DAYS?

In Figure 2 we can find a prominent peak at 23.69 days. By dividing the CMP dates of the northern hemisphere super active regions by 23.69 days, we can find that 7 out of the 9 northern hemisphere super active regions fall in the phase interval 0.08–0.12, which is very narrow. The S value of the peak at 23.69 days is 16. Following the Monte Carlo simulations, this peak is significant at about a 3.7σ level. In Figure 7 we also find a prominent peak at 23.86 days, which is significant at about a 2.5σ level.

The histograms in Figure 11 show flare distributions in frames rotating with periods 23.69 days and 23.86 days, for the northern and southern hemispheres respectively. We can find one zone of flare concentration for each hemispheres.

It is statistically very improbable that so many major flares fall in narrow longitudinal intervals, as shown above. It is also very improbable that the rotation periods are very close to each other by chance — 23.69 days for the northern hemisphere, 23.86 days for the southern hemisphere. These periods differ by only 0.8 %. Therefore, it is suggestive that the period of 23.78 ± 0.1 days may represent

a real rotation. There is no known surface rotation with this period. Hence, if it is a real rotation, it must be a rotation of active centers located deep inside the Sun. It is interesting to note that Knight, Schatten, and Sturrock (1979) found a periodicity of 12.07 days in their sunspot number analysis, which is about one half of 23.78 days.

VI. SUMMARY AND CONCLUSIONS

Important discoveries of the present paper are summarized as follows:

(1) A small number (28) of "super active regions" produced the majority of the major flares during the period from 1980 February to 1985 August. These super active regions are large, complex active regions containing large sunspots.

(2) There exist active zones, in which the flare occurrence rate is much higher. The longitudinal separation of the two active zones in the same hemisphere is about 180 degrees, and the active zones of the southern hemisphere are misaligned from those of the northern hemisphere by about 80 degrees. The rotation period of the active zones is 26.75 days. This period is very similar to the period one can deduce from the large scale magnetic polarity patterns of the equatorial strip of N20-S20 (McIntosh 1981). This period, however, is somewhat faster than a recent result for all sunspot groups by Howard, Gilman, and Gilman (1984) and that for photospheric gas flows by Scherrer, Wilcox, and Svalgaard (1980). The Carrington longitudes of active zones increase by 7.07 degrees per Carrington rotation. The active zones may be due to giant convection cells. The hierarchy of active centers can be represented as follows:

Sunspots \Rightarrow Active Regions \Rightarrow Activity Complexes \Rightarrow Active Zones

The lifetimes of these active centers increase with the hierarchy. For sunspots,

lifetimes are on the order of days; for active regions, tens of days; for complexes of activity, months; and for active zones, their lifetimes are several years.

(3) There is a hint of active centers rotating at a period of 23.7 days. It is possible that active centers in deep layers rotate with such a period.

This research was supported by NASA grants NGL 05-020-272 and ONR contract N00014-85-K-0111 at the Stanford University. The author has benefited from discussions with Drs. P. A. Sturrock, P. S. McIntosh, P. H. Scherrer, R. S. Bogart, and J. T. Hoeksema. This work could be performed timely because of prompt publication of the HXRBS event listing by the HXRBS group (P.I., K. J. Frost; Project Scientist, B. R. Dennis). The author commends their policy of sharing the HXRBS data with many scientists.

TABLE 1
CHARACTERISTICS OF SUPER ACTIVE REGIONS

NO.	ACTIVE REGION NUMBER ^a	NO. OF MAJOR FLARES ^b	CMP DATE	CMP TIME ^c	MAX. SPOT AREA ^d	A.R. CLASS	^e	^f	
1	16747 (2372)	8 (0)	80 Apr	7.3	97.3	1530	Eki	N	221
2	16815 (2418)	5 (1)	May	6.5	126.5	500	Eki	S	188
3	16923 (2522)	5 (0)	Jun	23.3	174.3	600	Eki	S	264
4	16978 (2562)	6 (1)	Jul	17.3	198.3	1080	Eki	S	301
5	17244 (2776)	11 (3)	Nov	6.6	310.6	1510	Ekc	N	230
6	17255 (2779)	16 (2)	Nov	11.6	315.6	2500	Fkc	S	163
7	17491 (2958)	6 (2)	81 Mar	2.8	426.8	1176	Dkc	S	106
8	17590 (3049)	7 (2)	Apr	20.7	475.7	1170	Dkc	N	168
9	17751 (3221)	5 (1)	Jul	24.2	570.1	2120	Dkc	S	338
10	17760 (3234)	9 (2)	Jul	28.3	574.3	2750	Fkc	S	281
11	17777 (3257)	7 (2)	Aug	10.0	587.0	2250	Fkc	S	110
12	17824 (3310)	5 (0)	Sep	4.9	612.9	S	122
13	17830 (3317)	10 (3)	Sep	10.6	618.6	N	45
14	17906 (3390)	12 (3)	Oct	14.3	652.3	1630	Ekc	S	311
15	17969 (3432)	5 (0)	Nov	4.9	673.9	2080	Fki	S	21
16	18176 (3576)	5 (1)	82 Feb	1.4	762.4	1330	Fkc	S	270
17	18201 (3594)	5 (0)	Feb	10.7	771.7	2600	Fkc	S	145
18	18280 (3659)	8 (1)	Mar	29.0	818.0	1210	Ekc	N	241
19	18405 (3763)	17 (6)	Jun	8.5	889.5	1160	Eki	S	359
20	18422 (3776)	15 (3)	Jun	18.8	899.8	3120	Fkc	N	221
21	18430 (3781)	7 (1)	Jun	21.5	902.5	1250	Eki	N	184
22	18474 (3804)	13 (4)	Jul	15.0	926.0	3350	Fkc	N	228
23	18473 (3814)	8 (0)	Jul	15.5	926.5	1210	Eki	N	221
24 (3994)	7 (1)	Nov	20.0	1054.0	1940	Eki	S	305
25 (4026)	5 (3)	Dec	16.9	1080.9	830	Dkc	S	303
26 (4171)	6 (2)	83 May	13.0	1228.0	970	Dko	S	124
27 (4474)	10 (2)	84 Apr	28.2	1579.2	3210	Fki	S	77
28 (4492)	11 (1)	May	24.5	1605.5	940	Fko	S	83

^a The first numbers are Hale active region numbers, and the numbers in parentheses are NOAA active region numbers. Hale active region numbers are no longer published in *SGD* after 1982 July.

^b Numbers in parentheses in this column indicate numbers of flares with HXRBS peak rates $\geq 10,000$ counts s^{-1} .

^c Central meridian passage dates after 00:00 UT on 1980 January 1.

^d Total spot area of the active region at the time of maximum. In millionth of the solar disk.

^e Hemisphere in which the active region is located.

^f Relative longitudes in a reference frame rotating with a 26.75-day period.

REFERENCES

- Bogart, R. S., and Bai, T. 1985, *Ap. J. (Letters)*, **299**, L51.
- Brandt, S. 1976, *Statistical and Computational Methods in Data Analysis*, 2nd ed., (Amsterdam: North-Holland Pub. Co.)
- Bumba, V., and Howard, R. 1965 *Ap. J.*, **141**, 1492.
- Bumba, V., and Obridko, V. N. 1969, *Solar Phys.*, **6**, 104.
- Carrington, R. C. 1863, *Observations of Spots on the Sun*, (London: Williams and Norgate).
- Dennis, B. R., Orwig, L. E., Kiplinger, A. L., Gibson, B. R., Kennard, G. S., and Tolbert, A. K., 1985, *The Hard X-Ray Burst Spectrometer Event Listing*, NASA TM-86236, (Washington, D.C.: NASA)
- Dodson, H. W., Hedeman, E. R., and Roelof, E. C. 1981, *World Data Center for Solar-Terrestrial Physics Report UAG-81*, (Boulder: NOAA).
- Gaizauskas, V., Harvey, K. L., Harvey, J. W., and Zwaan, C. 1983, *Ap. J.*, **265**, 1056.
- Howard, R., Gilman, P. A., and Gilman, P. I. 1984, *Ap. J.*, **283**, 373.
- Ichimoto, K., Kubota, J., Suzuki, M., Tohmura, I., and Kurokawa, H. 1985, *Nature*, **316**, 422.
- Kiplinger, A. L., Dennis, B. R., and Orwig, L. E. 1984, *Bull. A.A.S.*, **16**, S91.
- Knight, J. W., Schatten, K. H., and Sturrock, P. A. 1979, *Ap. J. (Letters)*, **227**, L153.
- McIntosh, P. S. 1981, in *The Physics of Sunspots*, ed. L. E. Cram and J. H. Thomas, (Sunspot: Sacramento Peak Observatory).
- . 1986, preprint.
- Rieger, E., Share, G. H., Forrest, D. J., Kanbach, G., Reppin, C., and Chupp, E. L. 1984, *Nature*, **312**, 623.

- Scherrer, P. H., Wilcox, J. M., and Svalgaard, L. 1980, *Ap. J.*, **241**, 811.
Solar-Geophysical Data, 1980 - 1985, (Boulder: NOAA).
- Svestka, Z. 1970, *Space Res.*, **10**, 797.
- . 1976, *Solar Flares*, (Holland: Reidel), ch. 5.
- Svestka, Z., and Simon, P. 1969, *Solar Phys.*, **10**, 3.
- Warwick, C. S. 1965, *Ap. J.*, **141**, 500.
- Weiss, N. O. 1964, *Mon. Not. Royal Astro. Soc.*, **128**, 227.

FIGURE CAPTIONS

- Fig. 1- Number of Active regions vs. number of major flares per active region. Two cases of the Poisson distributions are shown for comparison.
- Fig. 2- RMS deviation of the longitudinal flare distribution as a function of assumed rotation period, for the northern hemisphere. Peak *A* is at 26.75 days, and *B* at 23.69 days.
- Fig. 3- Longitudinal flare distribution for the northern hemisphere in a frame rotating with a period of 26.75 days.
- Fig. 4- Family trees of important active regions of the northern hemisphere. The assumed rotation period for this figure is 26.75 days. Four symbols are used to represent different types of active region: big solid squares represent super active regions; big solid circles, active regions observed to produce 3 or 4 major flares; small solid circles, active regions with 1 or 2 major flares; and small open circles, active regions without any major flares. For comparison, two slanted straight lines indicating the zero Carrington longitude is shown.
- Fig. 5- Same as Fig. 4, for the southern hemisphere.
- Fig. 6- Longitudinal flare distribution for the southern hemisphere in a frame rotating with a period of 26.75 days.
- Fig. 7- Same as Fig. 2, for the southern hemisphere. Peak *A* is at 26.78 days, and peak *B* at 23.86 days. Peak *C* at 26.28 days and peak *D* at 27.28 days are more prominent than peak *A*.
- Fig. 8- Family trees of important active regions appeared in the southern hemisphere. Similar to Fig. 5, but the *X*-axis represents the Carrington longitude.
- Fig. 9- Flare distribution in a frame rotating with a period 26.75 days.

- Fig. 10- Important active regions. Filled circles are southern hemisphere active regions, and open circles, northern hemisphere. Big circles represent super active regions, and small circles, active regions with 3 or 4 major flares.
- Fig. 11- Histograms for longitudinal flare distributions. Panel (a) for the northern hemisphere with an assumed rotation period 23.69 days, and panel (b) for the southern hemisphere with an assumed rotation period 23.86 days.

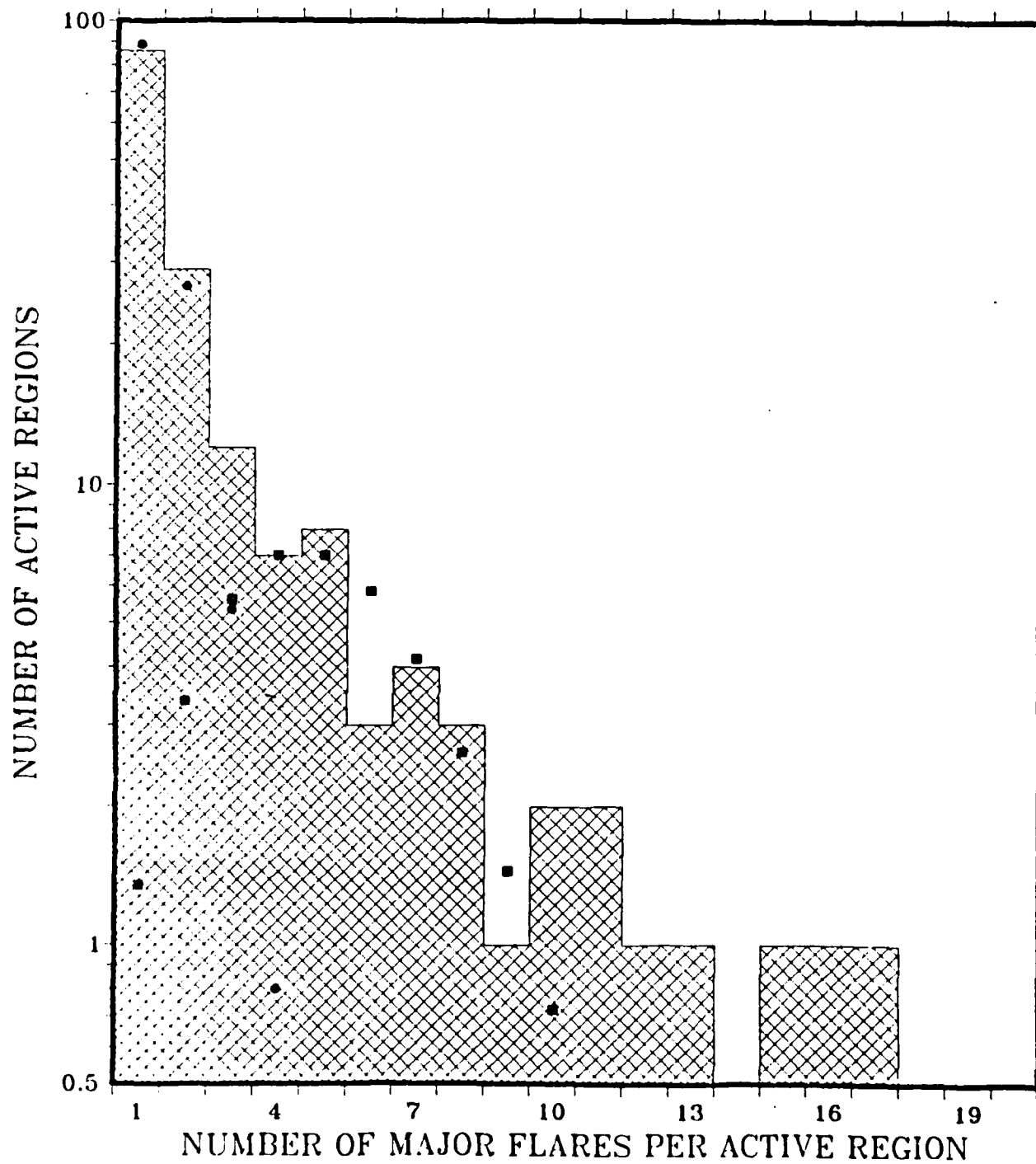


Fig. 1

ALPHA = 6 DEGREES

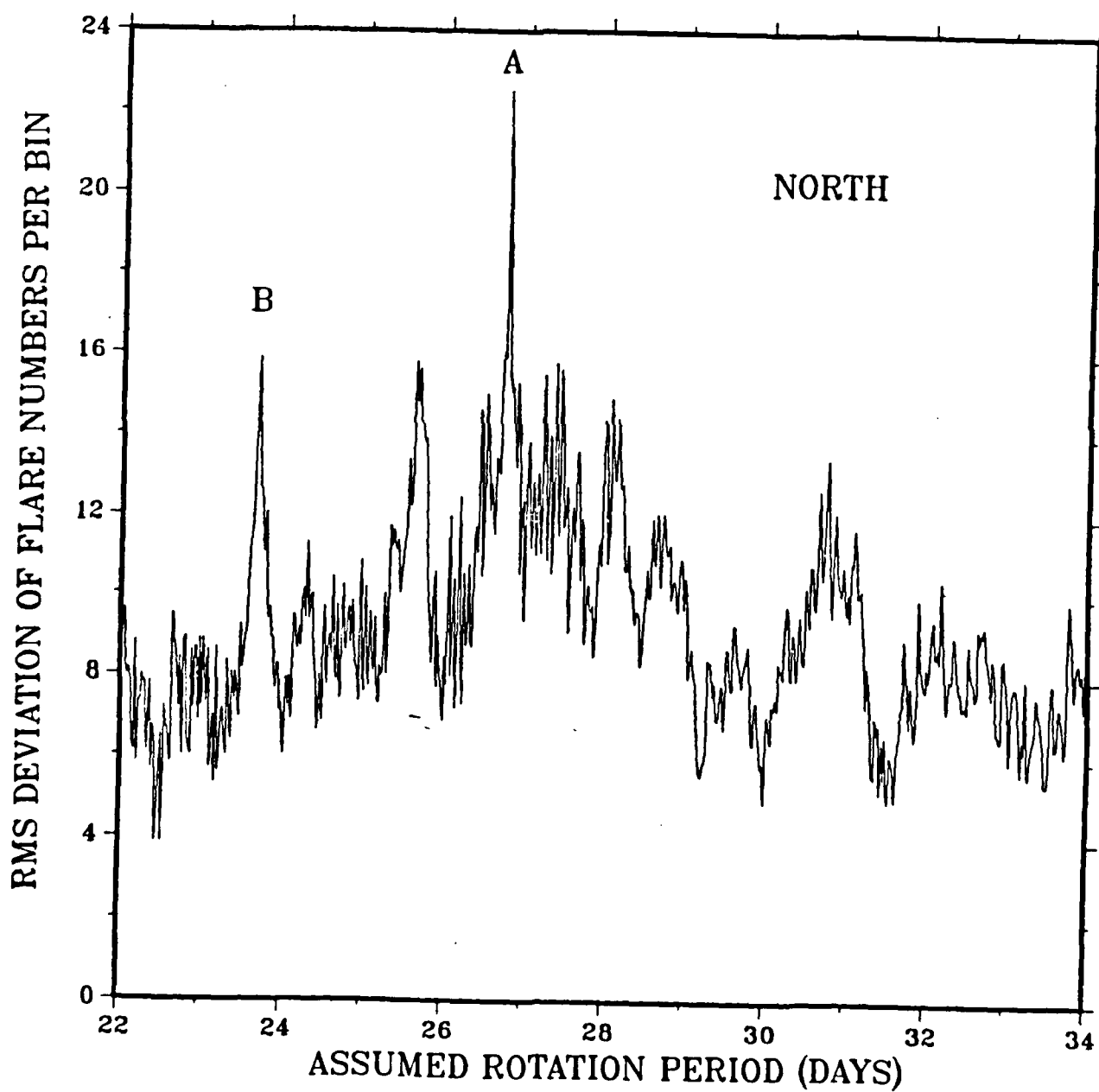


Fig. 2

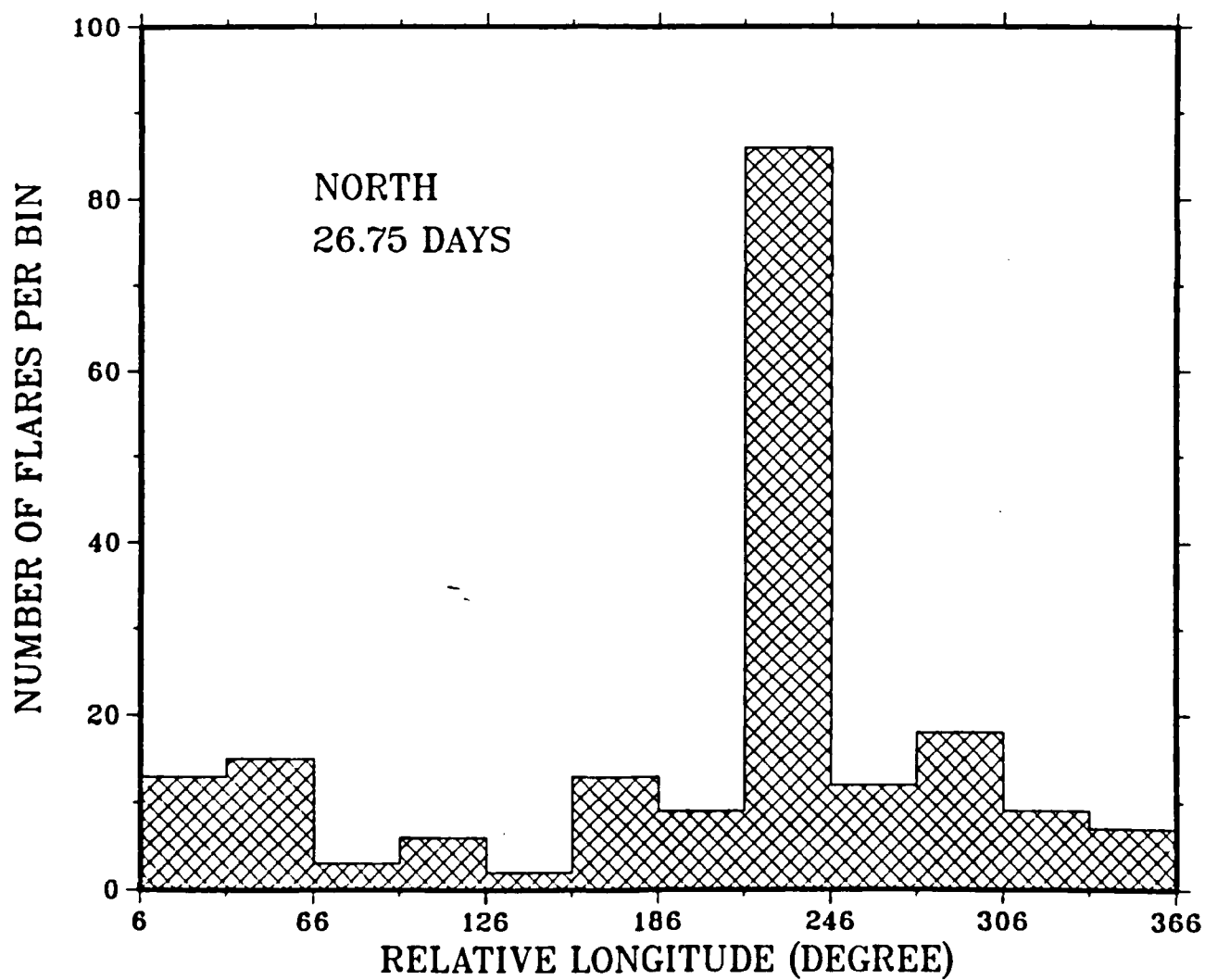


Fig.3

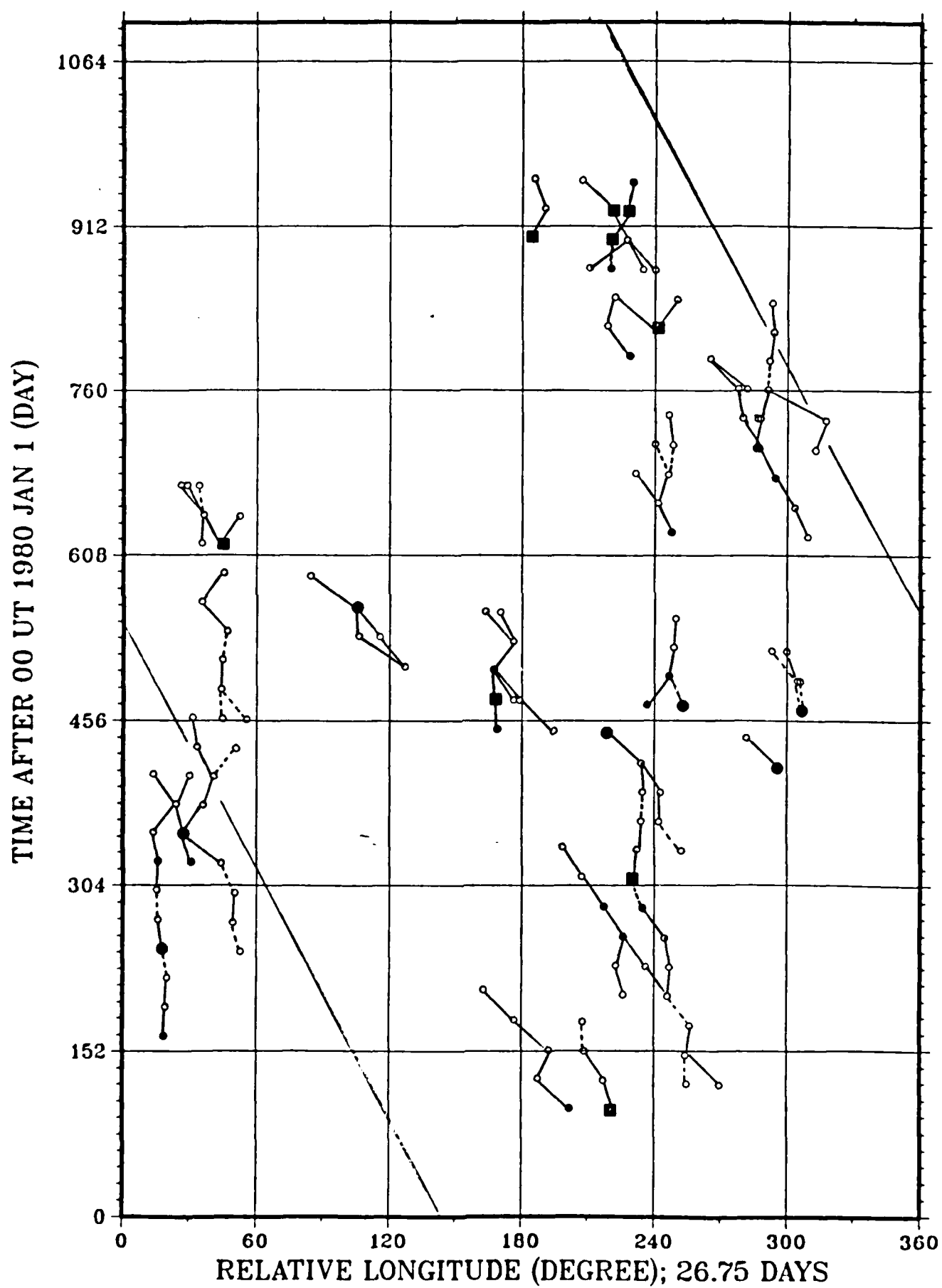
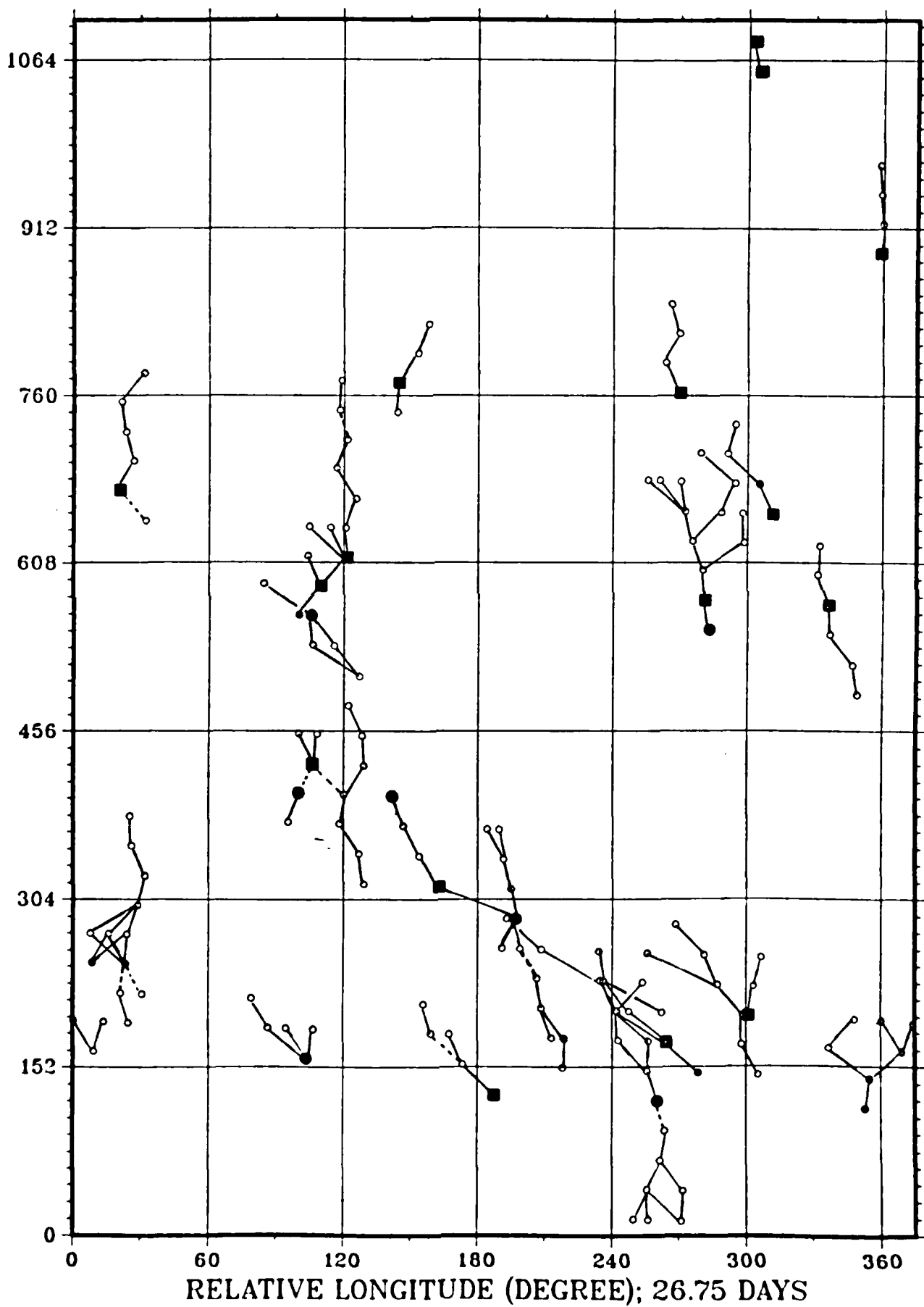


Fig. 4

TIME AFTER 00 UT 1980 JAN 1 (DAY)



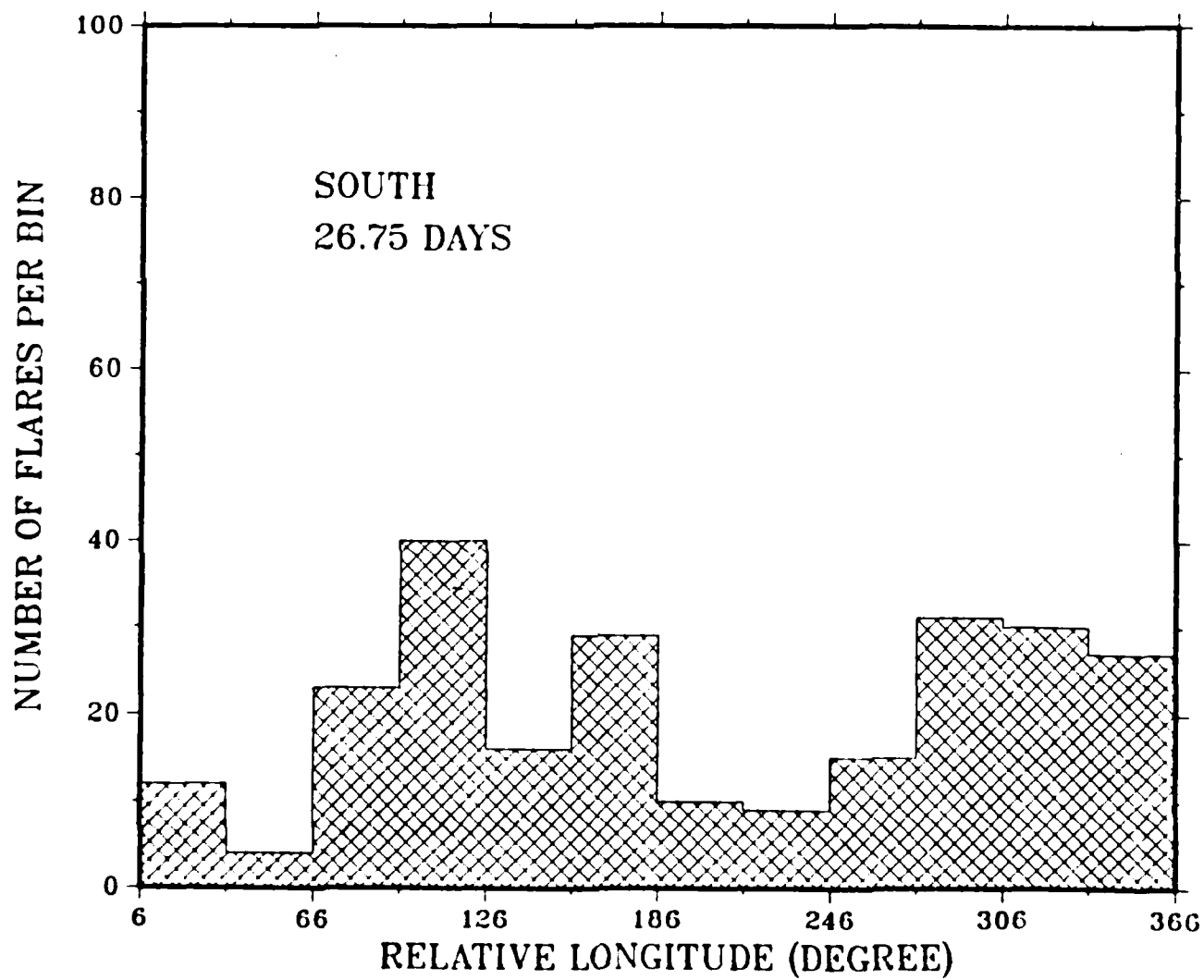


Fig. 6

ALPHA = 9 DEGREES

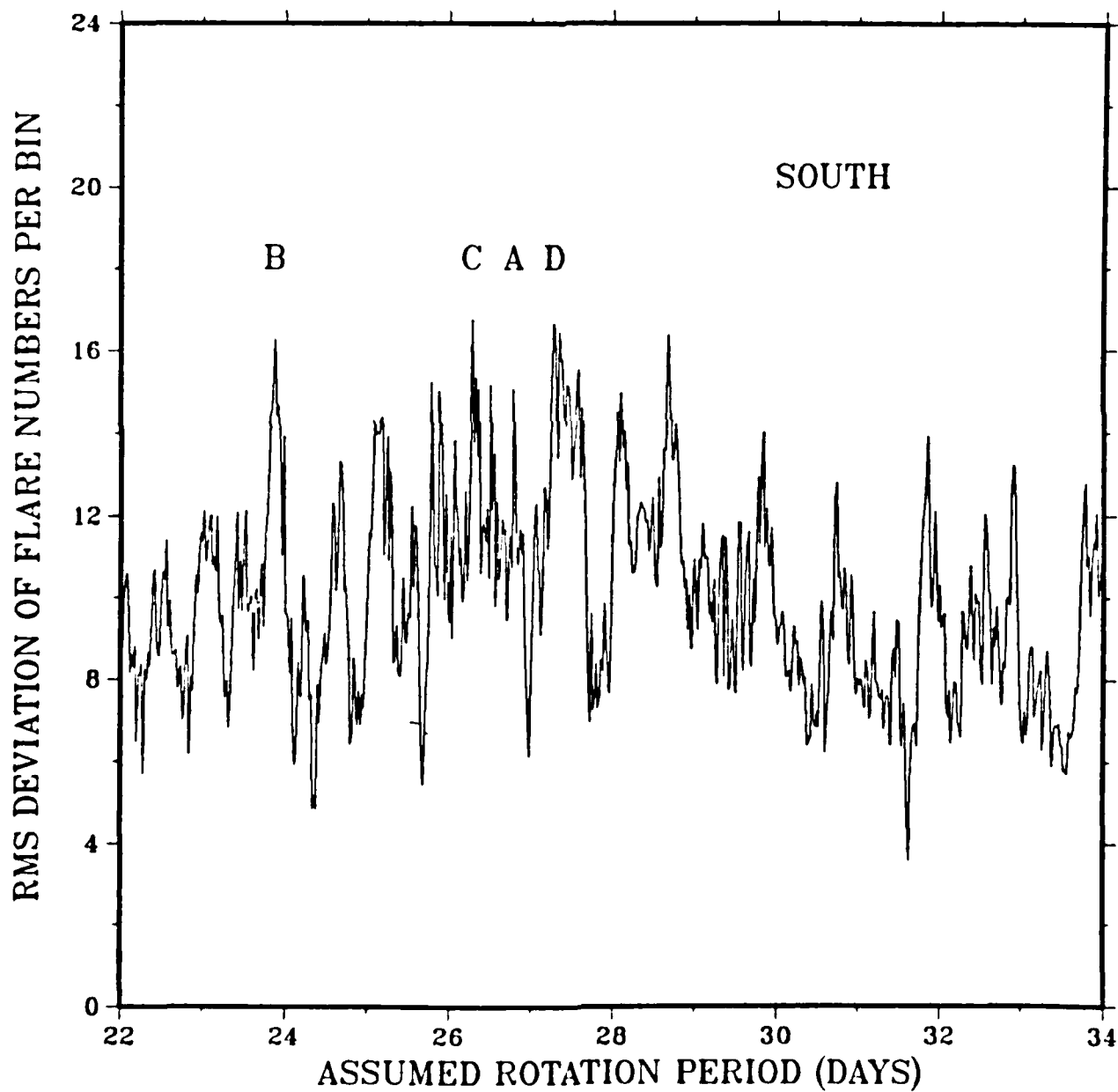
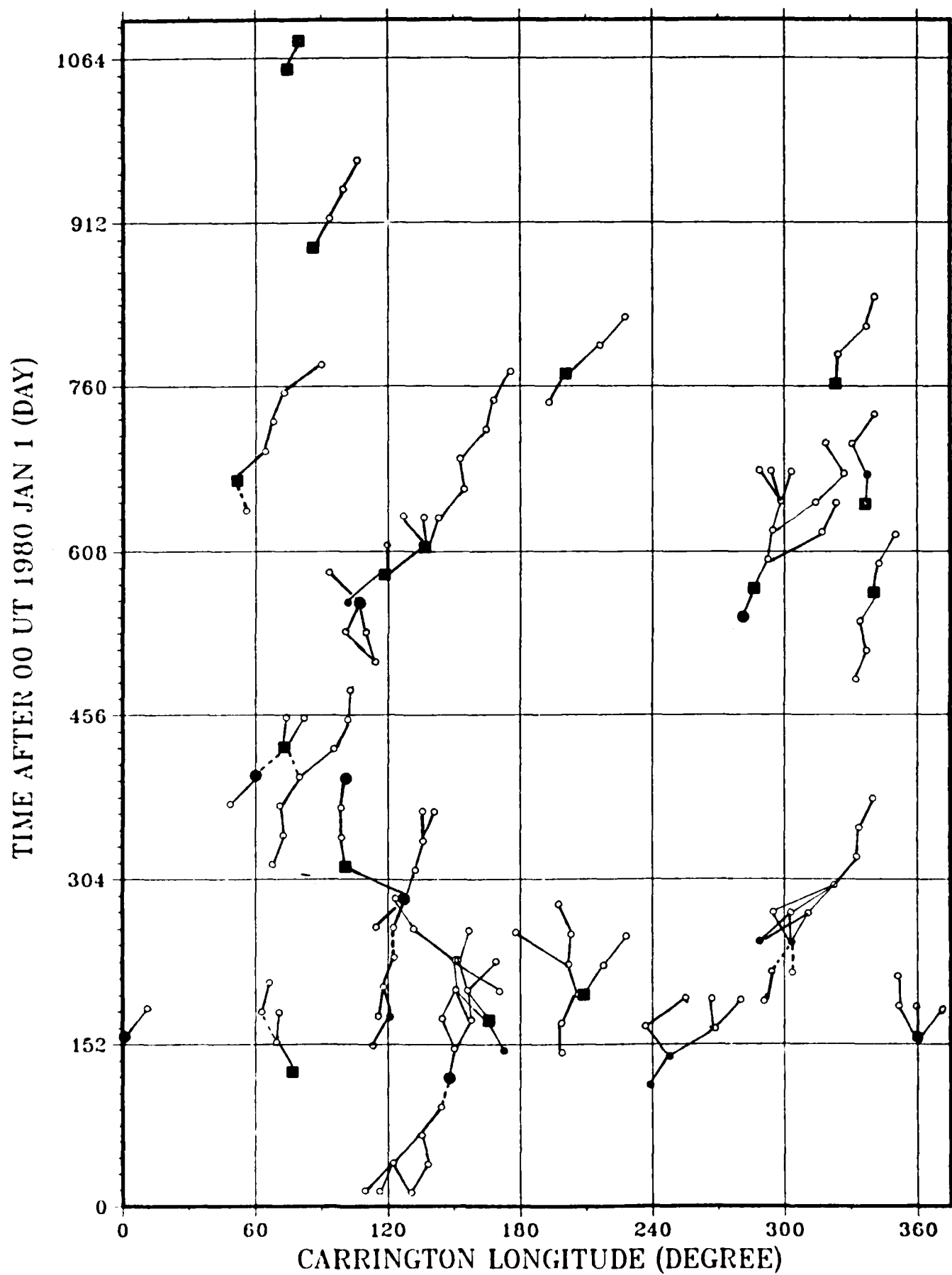


Fig. 7



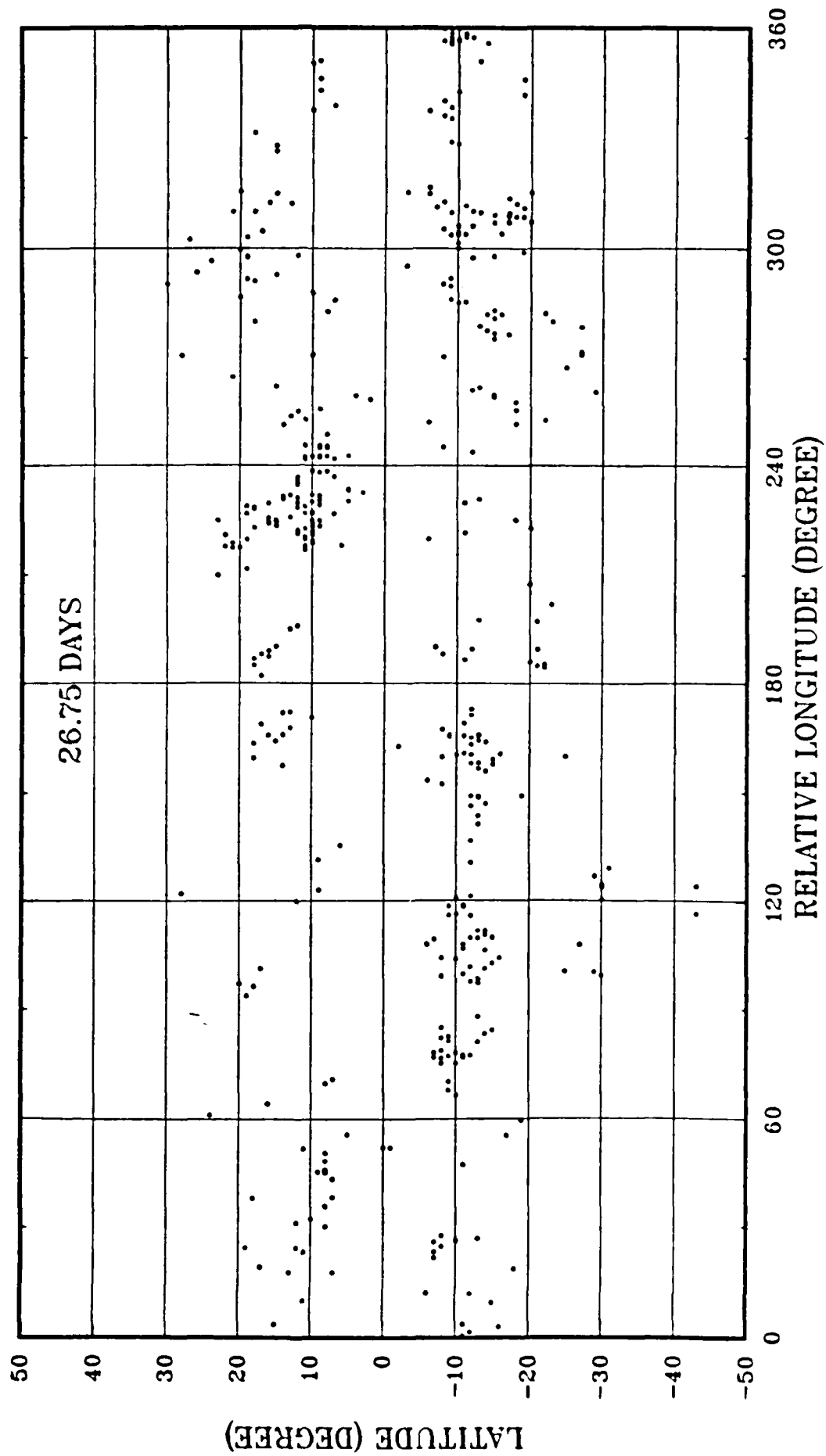
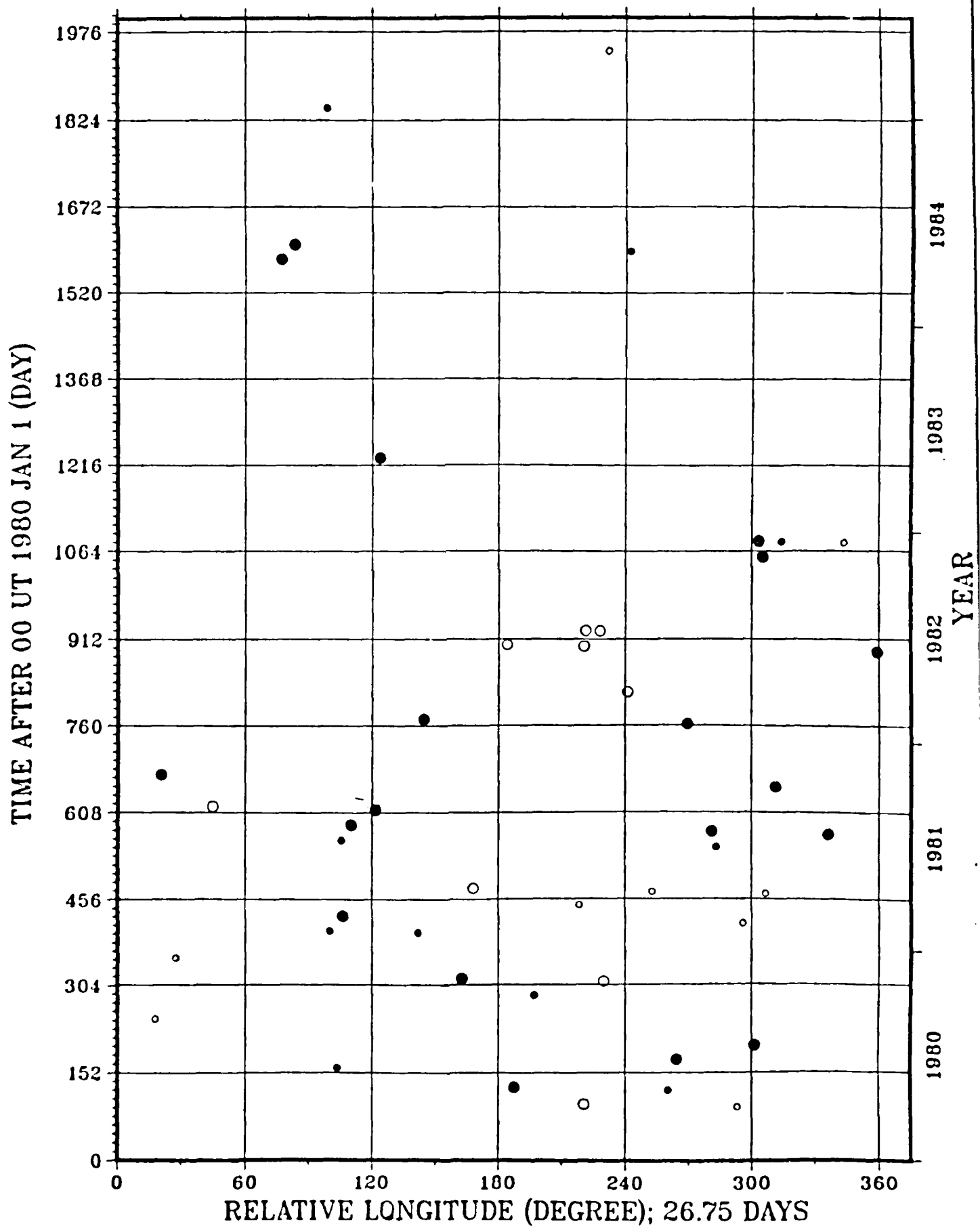


Fig. 9



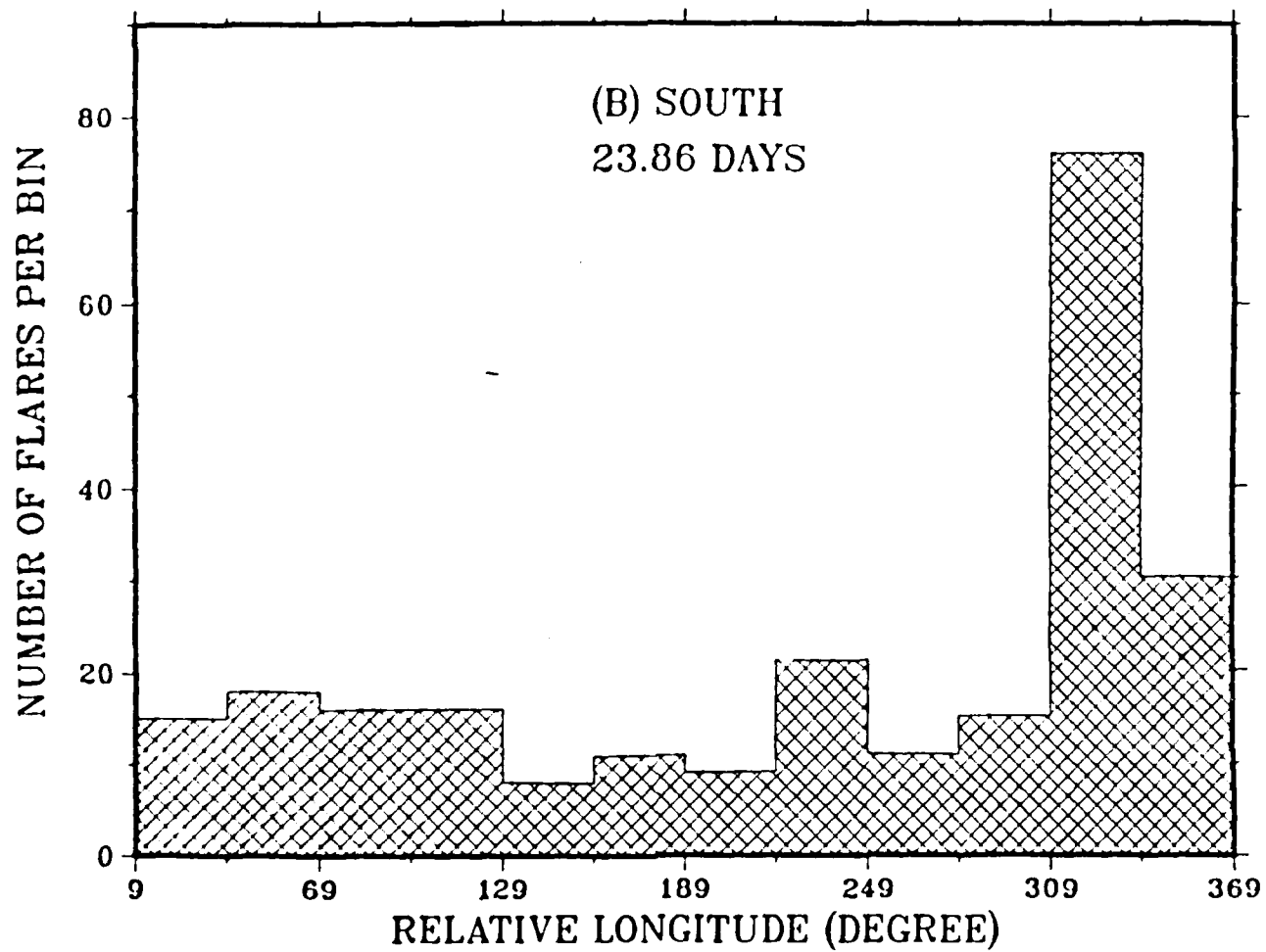
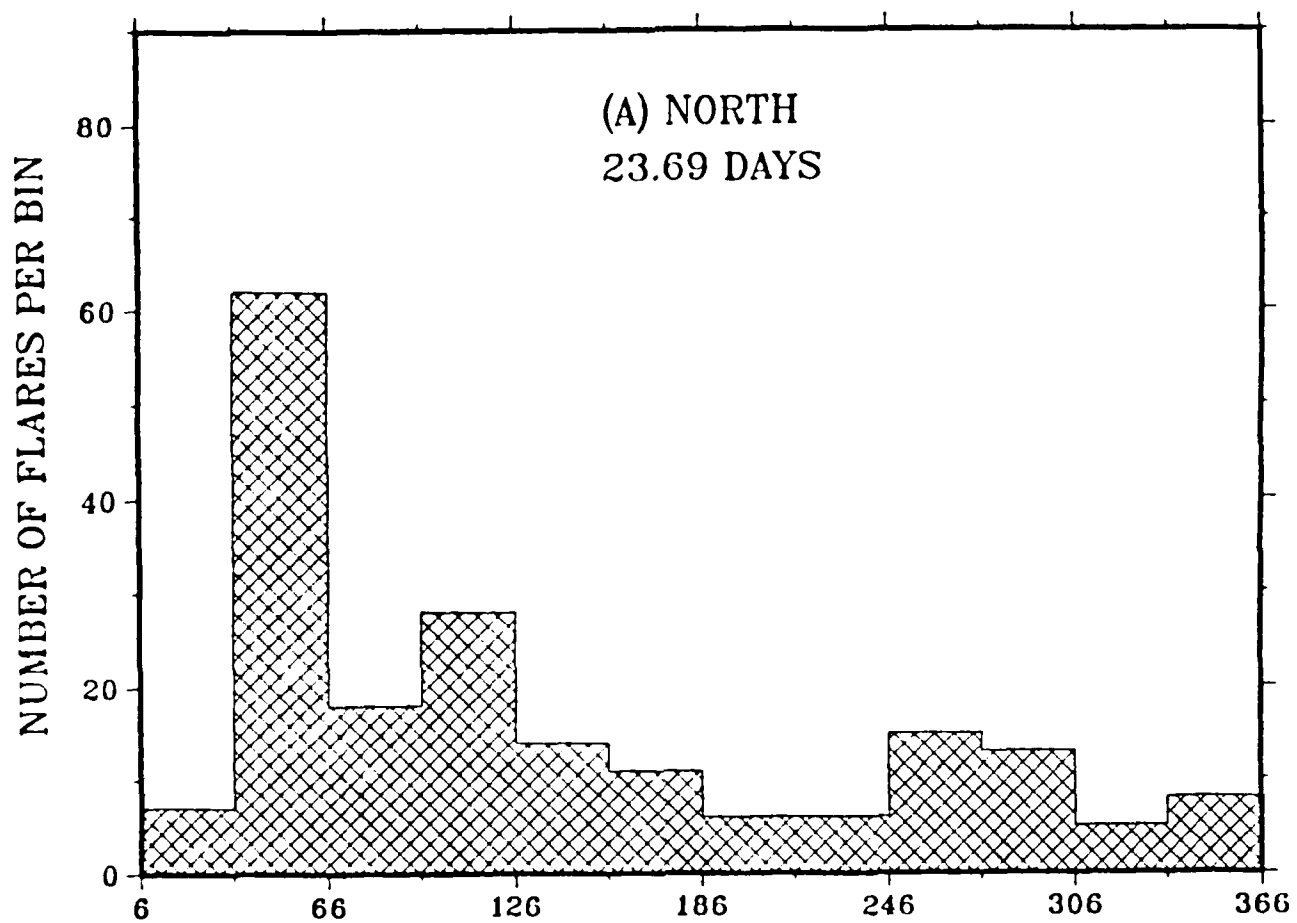


Fig. 11

END

2-87

DTIC